

Chemical sputtering of carbon by combined exposure to nitrogen ions and atomic hydrogen

M Schlüter, C Hopf and W Jacob¹

Max-Planck-Institut für Plasmaphysik, EURATOM Association,
Boltzmannstrasse 2, D-85748 Garching, Germany
E-mail: Wolfgang.Jacob@ipp.mpg.de

New Journal of Physics **10** (2008) 053037 (17pp)

Received 7 April 2008

Published 29 May 2008

Online at <http://www.njp.org/>

doi:10.1088/1367-2630/10/5/053037

Abstract. Chemical sputtering of amorphous hydrogenated carbon films by exposure to nitrogen molecular ions and combined exposure to nitrogen molecular ions and atomic hydrogen was studied as a function of ion energy in the range 30–900 eV and as a function of temperature between 110 and 350 K. The yield for nitrogen ions alone is substantially higher than that expected for physical sputtering. Furthermore, it shows only very weak variation with energy in the range from 900 down to 50 eV. This behaviour is interpreted as a clear indication of chemical sputtering. Combined exposure to nitrogen ions and atomic hydrogen causes substantially higher erosion yields than nitrogen alone and shows a distinct energy dependence. Reduction of the substrate temperature causes no measurable change of the chemical sputtering yields. Model descriptions are presented for the ions-only and ions-plus-hydrogen cases.

¹ Author to whom any correspondence should be addressed.

Contents

1. Introduction	2
2. Experimental	3
3. Results	4
3.1. Chemical sputtering by nitrogen ions only	4
3.2. Chemical sputtering by combined exposure to N_2^+ and atomic hydrogen	6
3.3. Chemical sputtering below room temperature	7
4. Modelling	8
4.1. A model for chemical sputtering by combined exposure to N_2^+ and atomic hydrogen	8
4.2. A model for chemical sputtering by nitrogen ions only	11
5. Summary and conclusions	14
References	15

1. Introduction

The theoretical prediction of Liu and Cohen [1] on a hypothetical covalently bonded β - C_3N_4 compound with a hardness higher than that of diamond spurred considerable efforts by many groups to synthesize hydrogen-free as well as hydrogen-containing carbon–nitrogen thin films (a–C:N and a–C:N:H, respectively) [2]. Many different methods have been used including plasma deposition [2]–[4], sputter deposition [5]–[11], ion beam deposition [12]–[15] and implantation of high-energy ions [16, 17]. A common result from a variety of different deposition techniques is that the maximal achievable nitrogen fraction in hydrogen-free C:N films is limited to about 30–40 at.% and that the deposition rate decreases with increasing nitrogen addition to the working gas [2, 18]. It was suggested that this is due to the formation of volatile CN species (e.g. C_2N_2) during the interaction of energetic nitrogen ions with the carbon surface [19]. Such a process is generally denoted *chemical sputtering* [20]. In the following years, characteristic signatures of chemical sputtering of carbon layers due to bombardment by nitrogen ions were reported [4, 5, 12, 17, 21, 22]. We have recently reported sputtering yields for the sputtering of a–C:H films with N_2^+ ions [23]. The energy dependence of this process differs significantly from physical sputtering and was therefore interpreted as a clear indication of chemical sputtering. In principle, the observations are very similar to the chemical sputtering of carbon by hydrogen ions [24, 25]. For a recent review of this process, see [20]. It was further shown that addition of hydrogen to the plasma leads to a substantial additional decrease of the achievable deposition rates [10, 15]. Depending on the actual condition at the sample surface, deposition of films can be completely suppressed [10, 15, 26] or even changed over to net erosion [26]. Chemical sputtering in the C/N/H system proceeds via formation of volatile species, such as hydrocarbons, HCN, CN and C_2N_2 [4, 5, 10, 17, 21, 22, 27, 28].

The interactions of nitrogen and hydrogen with carbon surfaces is also of interest in nuclear fusion research [29]. N_2 has been used as a candidate for impurity seeding in the divertor of tokamak experiments to reduce the local power load on highly exposed surfaces by enhanced radiative cooling [30, 31]. In addition, redeposition of carbon together with hydrogen isotopes is a challenge for the operation of any future device containing carbon as the first-wall material, because it will contribute significantly to tritium retention. To reduce redeposition in remote

areas of nuclear fusion devices, adding nitrogen in the divertor was suggested [29, 32]. However, in this instance, the combined interaction of nitrogen species (atoms and ions) and hydrogen with carbon surfaces has to be taken into account. Recently, Schwarz-Seelinger *et al* [26] have shown that chemical sputtering plays a very significant role in the etching of a-C:H films in hydrogen/nitrogen gas mixtures and during the deposition of a-C:N:H films in methane/nitrogen mixtures. These results are in excellent agreement with the earlier investigations of Nagai *et al* [33], who investigated the chemical sputtering of organic films in nitrogen and hydrogen containing plasmas for applications in integrated circuits production. The effect occurs only if the surface is bombarded with energetic species and the erosion rate has a maximum for a nitrogen fraction of about 20–30% [26, 33]. It is, therefore, of fundamental interest to nuclear fusion research to achieve a good understanding of the highly complex set of plasma–surface interaction processes in this system in order to be able to assess the consequences of N₂-seeding on carbon component lifetime and hydrogen inventory.

In this paper, we present sputtering yields for chemical sputtering of hydrocarbon layers by nitrogen molecular ions (N₂⁺) alone and by combined exposure to N₂⁺ and atomic hydrogen. The energy dependence was investigated in the energy range from 30 up to 900 eV. We further present the temperature dependence in the range from 340 K down to 110 K. A simple model for the energy dependence is presented and compared with the measured data.

Since there is no generally accepted definition of phrases such as chemical erosion and chemical sputtering, it is important to define how we will use them to avoid any confusion. Physical sputtering is the ejection of target atoms from a surface due to bombardment with an energetic projectile. It is a purely physical process which is dominated by momentum transfer between projectile and target atoms. Physical sputtering occurs for all projectile–target combinations. Sputtering may be enhanced or reduced if the projectiles form chemical bonds with the target atoms. Enhancement is due to the formation of volatile species. This process is generally called chemical sputtering [20]. But the sputtering yield may also be reduced if stable chemical compounds such as oxides or carbides are formed. In addition, chemically reactive species such as, e.g., hydrogen atoms can react with surface atoms and lead to the formation of volatile species. Such reactions are in general thermally activated and do not require physical momentum transfer. Consequently, such processes are called chemical erosion. We note that this definition differs from parts of the literature where chemical sputtering and chemical erosion are used synonymously. In the following, we will use the phrases physical sputtering and chemical sputtering, if we want to differentiate them from one another. The more general phrase sputtering will be used if either both processes are significant or if we cannot or do not want to distinguish between them. The phrase sputtering is preferred to the even more general phrase erosion, because it emphasizes the importance of ion energy for the process.

2. Experimental

The particle-beam experiments were carried out in the MAJESTIX device. The experimental setup is thoroughly described in [34]. In short: for the experiments described in this report the ion source and one radical beam source were used. A beam of mass-filtered ions was produced by a commercial Colutron G2-D low-energy ion-gun system. N₂⁺ ions were selected because the achievable ion currents were much higher than those for N⁺ ions. One of the radical beam sources is used to generate a flux of thermal, atomic hydrogen. Film thickness changes were measured in real time by ellipsometry. Because of the strong correlation of all physical

properties of the investigated hydrocarbon layers [35, 36], the carbon density of the layers can be determined from the measured optical constants. This allows converting the film thickness change into the number of eroded carbon atoms. With the measured impinging ion flux density, the erosion yields can be calculated from the sputtering rates. The yields in this paper are given as the number of eroded carbon atoms per impinging ion throughout, which means for nitrogen irradiation we give the yields per N_2^+ ion.

As samples, silicon wafers with approximately 30 nm thick a-C:H films were used. Amorphous hydrogenated carbon films were produced in the load lock of the MAJESTIX setup using an RF plasma with methane (CH_4) as a working gas [34]. Typical hard, diamond-like a-C:H films with a hydrogen content of $H/(H+C) \approx 0.3$ (with a refractive index of about 2, and a density of about 2 g cm^{-3}) were produced at a self-bias voltage of about 300 eV [35, 36].

The experimental capabilities of MAJESTIX in these experiments were extended over those described in [34]. Now, the substrate holder can be cooled by cold nitrogen gas to a minimum temperature of 110 K and heated resistively up to ≈ 900 K. The temperature of the a-C:H film is measured by a thermocouple clamped to the sample surface. In the cooling mode (T between 110 and 300 K), the temperature is held constant at the desired value by cooling with constant cooling power and controlled simultaneous heating.

The base pressure of MAJESTIX is 1×10^{-6} Pa. The background pressure increases to about 6×10^{-5} Pa, if the N_2^+ ion source alone is operational. During the operation of the atomic hydrogen source, it increases to about 4×10^{-4} Pa and if both the sources are running, it is about 5×10^{-4} Pa. The dominant contributions to the background during the operation of the particle-beam sources are molecular hydrogen and nitrogen, respectively. It was checked in separate experiments that these background contributions have no influence on the measured erosion yields.

3. Results

3.1. Chemical sputtering by nitrogen ions only

Figure 1 shows the sputtering yields for the bombardment of a-C:H films with N_2^+ ions and Ne^+ , respectively, that were already presented in [23]. The solid circles represent the measured sputtering yield for the bombardment with N_2^+ ions alone as a function of ion energy between 30 and 900 eV. The additional (compared with [23]) data point at 50 eV (square) was measured about 18 months after the series of original measurements along with the temperature series shown further below. In the meantime, the ion gun had been refurbished and the sample holder as well as the ellipsometer setup had been modified. The error bar for this data point is slightly lower than that of the original data because the new ellipsometer has a better accuracy than the former one. This data point demonstrates the good reproducibility of the absolute yields despite the modification of the experimental setup.

The data were thoroughly discussed in [23]. The results and interpretation are summarized here because they are the basis for further data and model results presented in this paper. The neon data (triangles) in figure 1 show a decrease in the physical sputtering yield with decreasing ion energy. They are in excellent agreement with predictions from TRIM.SP (dashed line). TRIM.SP [37] is a well-established Monte Carlo code based on the binary-collision approximation which allows a reliable calculation of physical sputtering yields. TRIM.SP correctly predicts the magnitude and energy dependence of the experimental results.

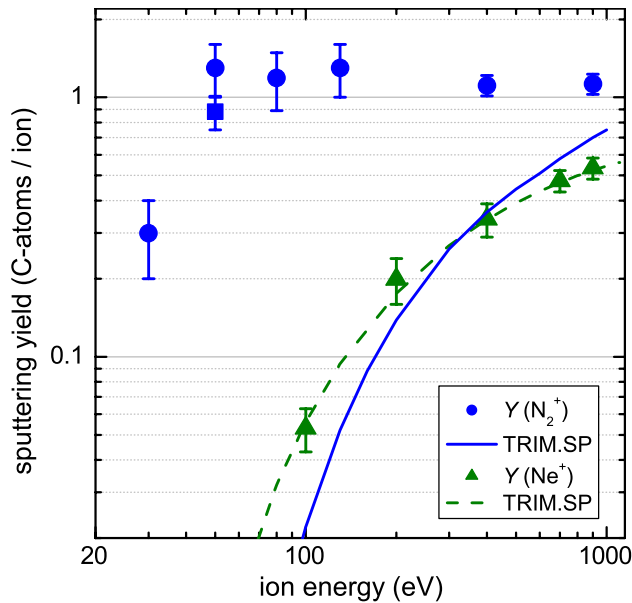


Figure 1. Chemical sputtering yield (eroded carbon atoms per incident N_2^+ ion) as a function of N_2^+ ion energy for bombardment of a-C:H films with N_2^+ ions (blue circles) ($j_{N_2^+} = (3.9 \pm 0.5) \times 10^{12} \text{ cm}^{-2} \text{ s}^{-1}$) (taken from [23]). The solid line is the physical sputtering yield calculated by TRIM.SP for a carbon surface binding energy of 2.8 eV. For comparison, the neon data (triangles) and TRIM simulations (dashed line) for physical sputtering with neon are also shown. The solid square at 50 eV marks an additional data point (compared with [23]).

The surface-binding energy of carbon for the TRIM.SP simulations was set to 2.8 eV, a value which was found to describe physical sputtering of such films with Ar^+ [38, 39], Ne^+ [39] and He^+ [40] ions very well.

The sputtering yield for N_2^+ ion bombardment is shown by the solid circles and the solid square. It is approximately constant taking on values in excess of 1 in the whole energy range 50–900 eV. Below 50 eV, it decreases strongly. The experimental data are compared with TRIM.SP simulations (solid line in figure 1). Because TRIM.SP cannot treat molecular ions, it was assumed that an N_2^+ ion behaves like two independent N^+ ions at half the energy. Clearly, this is an assumption which becomes questionable at low ion energies. This will be a topic of further research. At higher ion energies, this assumption appears to be justified and is commonly applied in the literature [20]. The surface-binding energy of the N^+ projectiles, which adds to the initial ion energy upon approach to the surface, was taken as 1.0 eV [41].

It is quite obvious that the N_2^+ data cannot be described by the TRIM.SP simulation results (solid line in figure 1). Neon was chosen for this comparison because its mass is very similar to that of nitrogen, so that the collision cascade physics for both the species should be rather similar. For example, the maximum transferable energy fraction in a binary collision is 0.994 for nitrogen and 0.938 for neon. The following differences between the neon and nitrogen results are found: the neon sputtering yield shows a clear energy dependence. In the investigated range, it decreases with decreasing ion energy by about one order of magnitude and agrees very well with the TRIM.SP simulation results. For energies below about 100 eV, the yield is negligible. Although TRIM.SP predicts very similar results for both species, the N_2^+ data are higher

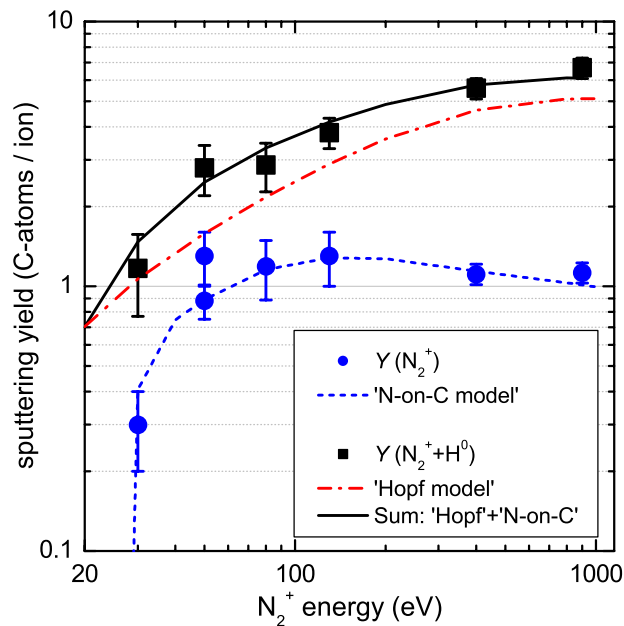


Figure 2. Chemical sputtering yield due to the combined bombardment of a-C:H films with N_2^+ ions and atomic hydrogen (black squares) and due to N_2^+ ions alone (blue circles) as a function of the N_2^+ ion energy ($j_{N_2^+} = (3.9 \pm 0.5) \times 10^{12} \text{ cm}^{-2} \text{ s}^{-1}$ and $j_{H^0} = (1.5 \pm 0.1) \times 10^{15} \text{ cm}^{-2} \text{ s}^{-1}$, $R = 380\text{--}400$, $T = 340 \text{ K}$). The blue dashed line shows the ‘N-on-C’ model (2), the red dashed–dotted line the Hopf model (1), and the black solid line the sum of the Hopf model and the ‘N-on-C’ model. The models are discussed in detail in section 4.

than the neon data in the whole energy range. In particular, below the threshold for physical sputtering $\approx 100 \text{ eV}$, the N_2^+ yield remains high. This discrepancy between the measured energy dependence for neon and nitrogen is a clear indication that chemical sputtering dominates a-C:H sputtering by nitrogen ions at low energies in close analogy to pure hydrogen-ion bombardment of graphite [20, 24, 25, 42]. Sputtering yields for hydrogen and deuterium bombardment of carbon materials also show a distinct deviation from TRIM.SP predictions at low energies. While TRIM.SP predicts a strong decrease of the yield for energies below about 100 eV, the measured yield remains rather constant for hydrogen and increases slightly for deuterium [24, 25]. The assumption that nitrogen bombardment of carbon surfaces is dominated by chemical sputtering is in agreement with the preceding mass spectrometric investigations which show the production of C_xN_y compounds [4, 5, 12, 17, 21, 22].

3.2. Chemical sputtering by combined exposure to N_2^+ and atomic hydrogen

Figure 2 shows a comparison of the chemical sputtering yield for bombardment with nitrogen ions alone and for the combined bombardment with N_2^+ and hydrogen. The following particle flux densities were used: $j_{N_2^+} = (3.9 \pm 0.5) \times 10^{12} \text{ cm}^{-2} \text{ s}^{-1}$ and $j_{H^0} = (1.5 \pm 0.1) \times 10^{15} \text{ cm}^{-2} \text{ s}^{-1}$, so that the hydrogen-to-ion flux ratio, R , was between 380 and 400. The yield for the combined bombardment case is higher than the yield for the nitrogen-only case in the whole energy range. Furthermore, the $N_2^+ + H^0$ case shows a much stronger energy dependence. The difference between the two cases increases with increasing energy. This measured energy

dependence for N_2^+ and hydrogen is in good agreement with other co-bombardment experiments using Ar^+ [38, 39, 43], Ne^+ [39] and He^+ [40] ions.

The observation of enhanced erosion in the presence of hydrogen is in agreement with published results for the deposition and erosion of C:N:H films using plasmas. As discussed in the introduction, Nagai *et al* [33] and Schwarz-Selinger *et al* [26] found that erosion in mixed hydrogen/nitrogen plasmas is much more efficient than in pure plasmas of these two gases. Unlike in our particle-beam experiments in plasmas, such an effect could at least partially be due to changes in the plasma parameters. For example, Nagai *et al* [33] found that in their inductively coupled plasma reactor the plasma density and, as a consequence, also the particle flux to the surface, increases significantly if nitrogen is added to a pure hydrogen plasma. On the other hand, Jacob *et al* [44] have shown that nitrogen addition to an electron-cyclotron resonance plasma leads to an decrease of the ion flux to the surface. Nevertheless, measured erosion rates increase significantly, indicating a strongly enhanced efficiency of chemical sputtering. Hellgren *et al* [10] investigated the deposition of a-C:N:H films by magnetron sputtering in $N_2/Ar/H_2$ atmosphere and found that the deposition rate decreases with increasing hydrogen admixture. For hydrogen fractions higher than about 15%, no film deposition was possible. Hammer *et al* [15], who studied the ion beam deposition of a-C:N:H films, also reported a decreasing deposition rate with increasing hydrogen addition. It is, however, very difficult to extract basic information about microscopic processes from such plasma and ion-beam experiments. The data presented in figure 2 clearly demonstrate that the combined interaction of N_2^+ and H^0 leads to much higher chemical sputtering yields than N_2^+ ion bombardment alone. They therefore provide a basis for the understanding of these experimental observations. Increasing hydrogen admixture increases the efficiency of chemical sputtering and decreases the observable net deposition rate. In some cases, deposition can be completely suppressed [10, 15] or even switched to net erosion [26].

3.3. Chemical sputtering below room temperature

The temperature dependence of the chemical sputtering yield for N_2^+ alone as well as $N_2^+ + H^0$ is presented in figure 3. The temperature was varied between 110 and 340 K. In the case of N_2^+ , the temperature dependence is shown for two ion energies, 50 and 400 eV. For both energies no dependence on temperature is observed in the investigated range.

In the $N_2^+ + H^0$ case, also we find no distinct temperature dependence. Only for the highest temperature measured here (340 K), is a small increase visible. This is in the same temperature range where chemical sputtering for noble gas ions plus H^0 starts to show an increase [40, 45] and is attributed mainly to the temperature dependence of the hydrogen-carbon chemistry.

The absence of a clear temperature dependence in the low temperature range is remarkable because condensation of C_2N_2 species was suggested to be responsible for a significant increase in the net deposition rate of a-C:N films [46]. Neidhard *et al* [46] deposited a-C:N films by magnetron sputtering in N_2/Ar mixtures. A sample bias of -25 V was used to assure low-energy ion bombardment during deposition. Investigating the carbon- and nitrogen-incorporation rates as a function of temperature they found an increase for both species with decreasing temperature. During the warm-up of films deposited at 140 K, they measured a strong increase of the C_2N_2 partial pressure in the chamber as the substrate reached 158 K, the sublimation temperature of C_2N_2 . They interpreted this observation as an incorporation of otherwise volatile C_2N_2 species in the growing film which are released if the sample temperature is increased above

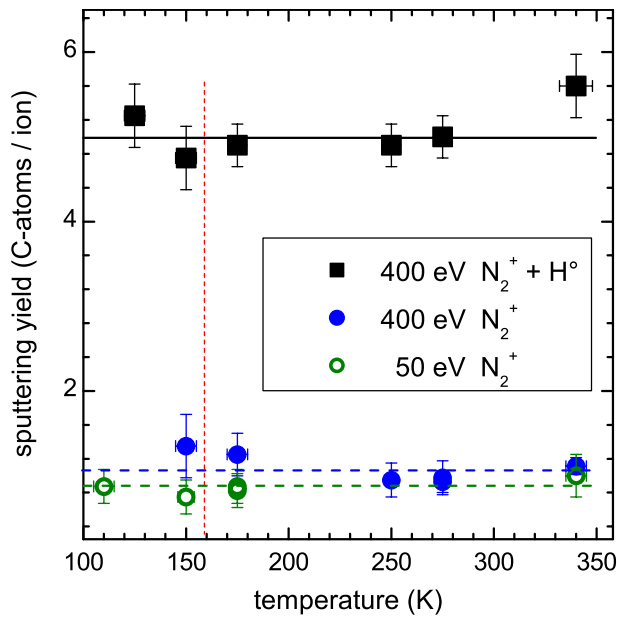


Figure 3. Chemical sputtering yield due to the combined bombardment of a-C:H films with N_2^+ ions and atomic hydrogen (black squares) and due to N_2^+ ions alone (blue circles) as a function of temperature (N_2^+ ion energy = 400 and 50 eV). The dashed vertical line at 158 K marks the condensation temperature of C_2N_2 which is a dominant erosion product. Particle flux densities are identical to those used in figure 2.

the sublimation temperature. Applying this interpretation to our case of chemical sputtering we would anticipate a decrease in the chemical sputtering yield at a temperature below 158 K, because C_2N_2 would not desorb by thermal activation. This is, however, not observed.

In recent investigations of the co-bombardment of a-C:H with argon ions and water [47] as well as molecular oxygen [48], we found an increase of the yield with decreasing sample temperature. In both cases, this is attributed to a chemical reaction between weakly adsorbed species and carbon atoms in the film being induced by impinging ions. The surface coverage with these weakly adsorbed species is controlled by a temperature-dependent adsorption–desorption equilibrium. The coverage increases with decreasing temperature, so that the yield for this process increases too. A comparable increase was, however, not observed for co-bombardment of a-C:H with argon ions and atomic hydrogen [40, 45] and, as shown in figure 3, neither for N_2^+ alone, nor for $N_2^+ + H^0$. Obviously, neither the hydrogen nor the nitrogen-driven processes in these surface reactions show an enhancement due to an adsorbed layer.

4. Modelling

4.1. A model for chemical sputtering by combined exposure to N_2^+ and atomic hydrogen

Hopf *et al* [38] devised a model to describe the energy dependence for the combined irradiation case which is based on the following microscopic mechanism: (i) incident ions break C–C bonds within their penetration range leaving behind dangling bonds. (ii) Atomic hydrogen, which is known to penetrate roughly 2 nm into a-C:H [49, 50], passivates the dangling bonds before they

recombine otherwise. (iii) Repetition of steps (i) and (ii) finally leads to the formation of volatile hydrocarbons below the surface, which diffuse to the surface and desorb. The latter process is assumed to be thermally activated. In the following, we will denominate this model as the ‘Hopf model’.

According to the Hopf model, the chemical sputtering yield is given by the integral over two depth-dependent factors: (i) the yield $y_{bb}(x)dx$ at which ions break C–C bonds at an interval dx and a depth x below the surface and (ii) a function which restricts this process to a near-surface layer. This function was chosen as an exponentially decaying function $\exp(-x/\lambda)$ with a characteristic decay length λ [38]. It was already discussed in [38] that there are two possible interpretations of λ . The original interpretation of Hopf *et al* was that λ describes the penetration range of atomic hydrogen into the surface of the a–C:H films. The alternative explanation was that λ represents the depth-dependent probability of the out-diffusion of erosion products formed at depth x . Initially, Hopf *et al* favoured the interpretation of λ as the range of atomic hydrogen in the a–C:H material, because the choice of $\lambda = 0.4$ nm which resulted in good agreement between the model and the data is in agreement with experimentally determined values for the penetration range of atomic hydrogen [49, 50]. But the successful adaptation of this model to the case of hydrogen-ion bombardment of graphite [42] favoured the alternative interpretation, since in this case there is no atomic hydrogen which has to penetrate the target. Taking into account the absence of a strong temperature dependence found in this work (figure 3) and for co-bombardment of a–C:H with argon ions and atomic hydrogen [40, 45], it is questionable whether this last step (migration to the surface) should be called diffusion. For a classical diffusion process, we would anticipate a significant temperature dependence in the investigated temperature range. It is also conceivable that the migration of molecules formed at the end of the ion range to the surface as well as the desorption step are both activated by following ion impacts. In this sense, we interpret the factor $\exp(-x/\lambda)$ simply as a depth-dependent probability for a formed molecule to leave the sample and refrain from giving an explicit physical interpretation of the underlying process.

The yield $y_{bb}(x, E)$ is determined from TRIM.SP [37] calculations for a given ion energy E counting the number of events where in a binary collision at least an energy E_{bb} is transferred to a carbon atom in the film. E_{bb} is interpreted as the minimum amount of energy that has to be transferred to a target carbon atom to break a C–C bond. It is chosen within the range of typical C–C bond energies in hydrocarbon molecules as 5 eV. One obtains

$$Y = a \int y_{bb}^C(x) \exp(-x/\lambda) dx, \quad (1)$$

where a is a scaling factor. Fitting this model to the cases Ar^+ and H^0 gave $a = 0.4$ as the scaling factor [38]. Recent investigations with improved experimental accuracy and a much broader database resulted in $a = 0.5$ [40]. This value for a yields an excellent description of the energy dependence for co-bombardment cases using Ar^+ , Ne^+ and He^+ [40] (see figure 4).

We apply here the same model with $a = 0.5$ to describe the energy dependence for the N_2^+ plus H^0 case. As for the N_2^+ ion-only case, we treat the N_2^+ ions in TRIM.SP as two N^+ ions at half the energy. The result of this model is shown as a dashed–dotted line in figures 2 and 4. Obviously, the agreement with the data is not satisfactory. In the whole investigated energy range, the measured yields are systematically higher than the model results. The agreement with the experimental data could be improved by increasing a to 0.65. However, considering the fact that the data for He^+ , Ne^+ and Ar^+ plus H^0 are well described by $a = 0.5$, and keeping

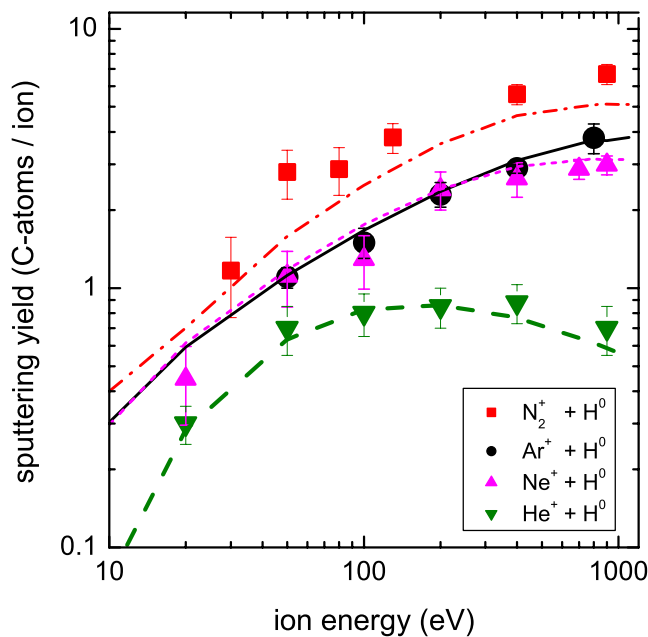


Figure 4. Chemical sputtering yield (eroded carbon atoms per incident ion) as a function of ion energy for the chemical sputtering of a-C:H films due to combined bombardment with atomic hydrogen and different ion species (N_2^+ , Ar^+ , Ne^+ and He^+) compared with the Hopf model according to (1). The ion-to-neutral flux ratio was between 340 and 360 for the noble gas plus H^0 and between 380 and 400 for the N_2^+ plus H^0 experiments. The sample was at a temperature between 320 and 340 K.

in mind that the collision cascade should be very similar for neon and nitrogen, such an increase of the scaling factor seems unjustified. Furthermore, even with an increased scaling factor the dependence at lower energies would not be very well described. Naturally, the slightly different trend at the lower energies could be an indication that the description of an N_2^+ ion by two N^+ ions breaks down at these low energies, as mentioned earlier.

We compare the data to a simple alternative model: assuming that the collision cascade physics which is responsible for the breaking of C–C bonds and the following interaction with atomic hydrogen is not affected by the chemical nature of the ion, we can still calculate this part of the process using the Hopf model with the scaling parameter $a = 0.5$. This assumption is reasonable because the chemical identity of a projectile is not important as long as the projectile is fast and the interaction is dominated by nuclear interaction. But at the end of the ion range, when the projectiles are decelerated to thermal energies, the projectile can interact chemically with the target atoms. If we further assume that this part of the interaction is identical to the N_2^+ -only case, then the total sputtering yield should be given by the sum of the Hopf model and the measured yields for N_2^+ -only. In the following section, we present a model for this interaction of N_2^+ ions with a-C:H layers. For simplicity, we will call this model ‘N-on-C model’. The sum of the Hopf model and the N-on-C model is shown in figure 2 as a solid line. The agreement with the data is excellent. In particular, the trend at the low energies, indicating a threshold energy in the range 10–20 eV, is reproduced better than with the simple Hopf model with an enhanced scaling factor of $a = 0.65$.

From this, we draw the following conclusions: both the processes are additive. N_2^+ ions produce broken bonds which react with atomic hydrogen. This part is well described by the Hopf model. In addition, at the end of the range the decelerated nitrogen atoms react with carbon (and maybe hydrogen) from the film to form additional volatile species which increases the measured sputtering yield compared with, e.g., the $Ne^+ + H^0$ case.

4.2. A model for chemical sputtering by nitrogen ions only

Recently, Hopf and Jacob [42] suggested a model to describe chemical sputtering of carbon by hydrogen ions. This model is based on the previously described model for the co-bombardment case (noble gas ions plus atomic hydrogen) presented in the preceding section [38] and was adapted to the case of bombardment with reactive ion species. The adapted model for the case of impinging reactive ions is based on the identical microscopic picture as the model for the co-bombardment case. As before, the reaction yield is proportional to the overlap of damage production and local hydrogen density. But in contrast to the co-bombardment case, the local density of hydrogen is now given by the implanted ions.

The impinging chemically reactive ions cause damage (broken bonds) in the near-surface layer. This is a purely physical effect driven by momentum transfer due to nuclear collisions of the projectiles with the target atoms. At the end of the ion range, when the ions are decelerated to thermal energies, they react chemically with the created broken bonds and form volatile reaction products. The probability for such a chemical reaction depends on the local density of the broken bonds and the density of reactive species. The density of the reactive species depends on the depth distribution of implanted projectiles. Only those reaction products formed within a certain distance from the surface can leave the solid and thus contribute to sputtering [42]. In addition to this chemical sputtering contribution, the impinging ions can cause physical sputtering if their energy is sufficiently high. According to this model, the total sputtering yield $Y_{\text{tot}}(E)$ is given by the sum of the physical ($Y_{\text{phys}}(E)$) and chemical ($Y_{\text{cs}}(E)$) sputtering yields,

$$Y_{\text{tot}}(E) = Y_{\text{cs}}(E) + Y_{\text{phys}}(E) = a \int y_{\text{bb}}(x, E) n(x, E) e^{-x/\lambda} dx + Y_{\text{phys}}, \quad (2)$$

where $y_{\text{bb}}(x, E)$ is the depth distribution of the produced broken bonds as a function of depth x and energy E and $n(x, E)$ is the depth distribution of the implanted projectiles. Both these depth distributions are calculated by TRIM.SP [37]. The term $\exp(x/\lambda)$ is the depth-dependent probability for the emission of erosion products formed at depth x . Finally, a is a scaling parameter. The details of the ion–solid interaction, in particular, the dependence on the projectile’s nature, mass and energy, are taken into account by the TRIM.SP calculations. Using this model, Hopf and Jacob [42] were able to describe the sputtering of carbon by hydrogen and deuterium ions reproducing many of the experimental details, in particular, the isotope effect between H and D.

We apply this model to the case of chemical sputtering of a–C:H films by N_2^+ ions (‘N-on-C model’). In these calculations, it is again assumed that an N_2^+ ion behaves like two N^+ ions at half the energy. As target for the TRIM.SP simulations, we again use an a–C:H film with an H/(H+C) ratio of 0.3 and a density of 2 g cm^{-3} . In [42], the following model parameters were used: a value of 5 eV was assumed as bond-breaking energy E_{bb} . The decay length for the emission probability of reaction products λ was set to 0.4 nm. A choice of $a = 1$ for the scaling parameter gave excellent agreement with the data. The surface-binding energy E_{SB} for graphite was set to 7.4 eV [37]. Because our target here is a–C:H (70% carbon and 30% hydrogen)

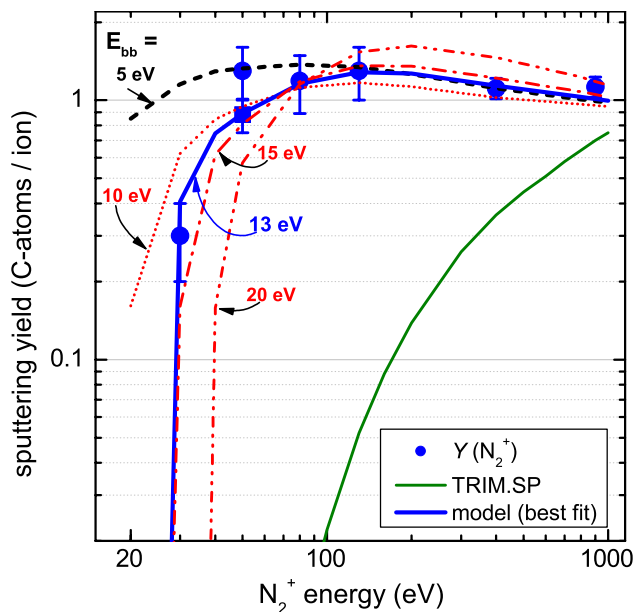


Figure 5. Sputtering yield as a function of ion energy for the chemical sputtering of a-C:H films due to bombardment with N_2^+ ions (symbols) compared with the model according to (2) for different choices of the parameter E_{bb} . TRIM.SP results which represent the contribution of physical sputtering are shown as a solid line labelled TRIM.SP.

and not graphite, we again apply $E_{SB} = 2.8$ eV (see section 3.1). Using otherwise the same parameters as in [42] for our case of N_2^+ ions, the agreement between the model and the data is very poor (see dashed line in figure 5). The agreement between the model and the data can be greatly improved if a higher value for E_{bb} is chosen. Figure 5 shows results of the model according to (2) for $E_{bb} = 5, 10, 13, 15$ and 20 eV. As the choice of the scaling parameter a is closely correlated with the choice of E_{bb} , different scaling factors have to be used for different choices of E_{bb} . This was discussed in [42]. A higher value of E_{bb} causes a lower number of broken bonds and, as a consequence, the scaling factor has to be increased to compensate for that. The values for a in figure 5 are chosen such that the chemical sputtering yield at energies above 50 eV is well described. The following pairs of parameters (E_{bb}, a) were used for the model curves shown in figure 5: (5 eV, 1.1), (10 eV, 2.2), (13 eV, 3.1), (15 eV, 4) and (20 eV, 7). All other parameters were held constant. Figure 5 shows that a choice of 13 eV for E_{bb} (solid line) yields excellent agreement with the measured data.

The best fit to the data is shown again in figure 6. In addition to the total sputtering yield (solid line), the contributions of chemical (dashed line) and physical (dashed-dotted line) sputtering are shown separately. The relative contribution of chemical sputtering decreases with increasing energy, but is significant in the whole investigated energy range. It is larger than the contribution of physical sputtering for energies lower than about 650 eV. Below about 200 eV, the sputtering yield is dominated by chemical sputtering.

We have presently no concluding explanation for the necessity to choose a different value for E_{bb} for the case of N_2^+ ion bombardment. One possible explanation is that for the involved nitrogen-carbon chemistry different types of damaged sites are required compared with the hydrogen-carbon chemistry and that the damage types for nitrogen need a higher transferred

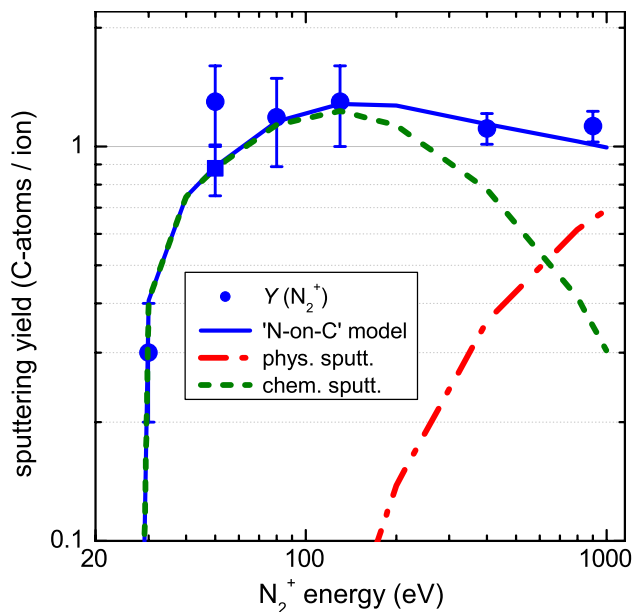


Figure 6. Sputtering yield as a function of N_2^+ ion energy for the chemical sputtering of a-C:H films due to bombardment with N_2^+ ions (blue circles) compared with the best fit for the model according to (2). The contributions of chemical sputtering and physical sputtering are shown separately.

energy. Another possible explanation is the significantly different bond energy (bond strength) of the used molecular ions. The H–H bond strength is 4.51 eV, and the N–N bond strength is 9.79 eV [51]. This energy has to be spent to dissociate the molecule upon impact. Since it requires more energy to break the N_2 molecule than the H_2 molecule, this could explain the higher threshold for N_2^+ ion bombardment. In this respect, it has to be noted that most data for chemical sputtering of carbon by hydrogen or deuterium were also measured using molecular ions (H_2^+ and H_3^+ and their deuterated equivalents) [20, 25].

It has been shown that for the case of hydrogen and deuterium on carbon at low energies, the measured yield per nucleon depends on the type of ion used. For the chemical sputtering of carbon by D^+ , D_2^+ and D_3^+ ions and energies below 60 eV per deuteron, the methane production yields per deuteron for the three different ion species start to deviate [52]–[55]. The difference between these yields increases with decreasing energy per deuteron. The yield for D_3^+ ions is always higher than that for D_2^+ , and that for D_2^+ ions is higher than that for D^+ ions. At an energy of 10 eV D^{-1} the D_3^+ yield is a factor of 2 higher than the D^+ yield. This effect of sputtering with molecular ions was first demonstrated by Yao *et al* [56], who investigated the physical sputtering of gold by N_2^+ and O_2^+ ions. An enhancement of the measured sputtering yield per atom for N_2^+ compared to N^+ was observed for energies below 500 eV per projectile (i.e. 250 eV per atom). The difference increased with decreasing ion energy. At 50 eV per atom, the N_2^+ yield is about a factor of 4 higher than the N^+ yield. For O_2^+ , they found similar enhancements over O^+ for energies below 100 eV per atom. Yao *et al* explained the higher value of the energy where the yields start to deviate for nitrogen compared with oxygen with the much higher bond strength of the N_2 molecule (9.79 eV [51]) compared with that for the O_2 molecule (5.16 eV [51]). So it is conceivable that the high bond strength of nitrogen causes deviations of the chemical sputtering yield at low energies observed in our experiments.

However, based on the available experimental data, we can presently not explain the higher threshold (E_{bb}) for nitrogen compared with hydrogen. This will require further dedicated experiments. Recently, we also found for the co-bombardment with argon ions and molecular oxygen [57] different behaviour compared with $\text{Ar}^+ + \text{H}^0$. In this case, the difference was also explained by the assumption that different types of damaged sites are involved in the underlying reactions.

5. Summary and conclusions

In summary, our investigations with the particle-beam experiment MAJESTIX show that bombardment of a-C:H layers with N_2^+ ions alone causes chemical sputtering. The sputtering yields (per N_2^+ ion) are surprisingly high; they are of the order of 1 for ion energies above 50 eV. The sputtering yield increases slightly with decreasing ion energy (in the range 900–100 eV) and decreases significantly below 50 eV. For this case of N_2^+ ions only, we adapted a model recently applied to the chemical sputtering of graphite by hydrogen ions only [42]. Applying this model, we achieved excellent agreement with the measured data, however, for changed model parameters. To yield good agreement with the experimental results, the bond-breaking energy had to be enhanced from 5 eV for H on C to 13 eV for N on C. The reason for this higher value presently remains unexplained.

Co-bombardment of a-C:H films with N_2^+ and H^0 results in enhanced chemical sputtering yields as observed earlier for noble gas ions plus H^0 [38, 39]. But the measured yields are even higher than those predicted by the Hopf model [38]. This is explained by the assumption that the two involved processes: (i) creation of broken bonds by the ions and reaction of these broken bonds with atomic hydrogen forming finally volatile hydrocarbon species and (ii) chemical interaction of the decelerated nitrogen atoms at the end of the ion range producing volatile C_xN_y or $\text{C}_x\text{N}_y\text{H}_z$ species, are additive, so that the yield predicted by the Hopf model is enhanced by the acting C–N–H chemistry.

Investigating the temperature dependence at cryogenic temperatures, we found no change of the chemical sputtering yield in the range from 340 down to 110 K. This is in contrast to recent observations for co-bombardment of a-C:H with argon ions and water [47] as well as molecular oxygen [48] which both showed an increase of the yield with decreasing sample temperature.

These experimental findings have some impact on the deposition of a-C:N and a-C:N:H films. As the measurable net deposition on plasma deposition is often the result of the competition between gross deposition and erosion, the high sputtering yields of nitrogen ions presented here are of relevance in the deposition of nitrogen-containing films from nitrogen-containing plasmas. The sputtering yields are quite high—of the order of 1 for N_2^+ only and $E > 50$ eV—and they are even higher in the presence of hydrogen. For the co-bombardment case, the yield increases with increasing ion energy. For mixed methane–nitrogen plasmas this can lead to a change over from deposition to erosion with increasing bias voltage, as was recently observed by Schwarz-Seelinger *et al* [26]. But even in a hydrogen-free plasma, the achievable net deposition rates will be strongly affected by the sputtering due to impinging nitrogen ions, which is much higher than the predictions for physical sputtering. These effects have to be taken into account for the modelling of such processes.

With respect to impurity-seeding of divertor plasmas in thermonuclear fusion experiments, it has to be noted that the bombardment of carbon surfaces with all impurity ions in a large

background of hydrogen will lead to high chemical-sputtering yields. The yields are high for argon and neon, but even higher (\approx factor of 2) for N_2^+ ions (see figure 4). To some extent, this higher yield for nitrogen is due to the additional erosion channel which leads to formation of volatile C_xN_y or $C_xN_yH_z$ species. In the end, the high erosion rates of target plates made of carbon-based materials might result in lifetime problems for these components.

References

- [1] Liu A Y and Cohen M 1990 Structural properties and electronic structure of low-compressibility materials: β - Si_3N_4 and hypothetical β - C_3N_4 *Phys. Rev. B* **41** 10727
- [2] Franceschini D F 2000 Plasma-deposited a-C(N):H films *Braz. J. Phys.* **30** 517
- [3] Rodil S E, Morrison N A, Robertson J and Milne W I 1999 Nitrogen incorporation into tetrahedral amorphous carbon *Phys. Status Solidi a* **174** 25
- [4] Hong J, Granier A, Goullet A and Turban G 2000 *In situ* deposition and etching process of a-C:H:N films in a dual electron cyclotron resonance–radio frequency plasma *Diamond Relat. Mater.* **9** 573
- [5] Hammer P and Gissler W 1996 Chemical sputtering of carbon films by low energy N_2^+ ion bombardment *Diamond Relat. Mater.* **5** 1152
- [6] Kaltofen R, Sebald T and Weise G 1996 Plasma diagnostic studies to the carbon nitride film deposition by reactive r.f. magnetron sputtering *Thin Solid Films* **290–291** 112
- [7] Kaltofen R, Sebald T and Weise G 1997 Low-energy ion bombardment effects in reactive rf magnetron sputtering of carbon nitride films *Thin Solid Films* **308–309** 118
- [8] Kaltofen R, Sebald T and Weise G 1997 Ion bombardment diagnostics in a nitrogen RF magnetron sputter discharge *Surf. Coat. Technol.* **97** 131
- [9] Baker M A, Hammer P, Lenardi C, Haupt J and Gissler W 1997 Low temperature sputter deposition and characterization of carbon nitride films *Surf. Coat. Technol.* **97** 544
- [10] Hellgren N, Johansson M P, Hjärvarsson B, Broitman E, Östblom M, Liedberg B, Hultman L and Sundgren J-E 2000 Growth, structure, and mechanical properties of CN_xH_y films deposited by dc magnetron sputtering in $N_2/Ar/H_2$ discharges *J. Vac. Sci. Technol. A* **18** 2349
- [11] Hellgren N, Johansson M P, Broitman E, Sandström P, Hultman L and Sundgren J-E 2001 Effect of chemical sputtering on the growth and structure of magnetron sputtered CN_x thin films *Thin Solid Films* **382** 146
- [12] Hammer P, Baker M A, Lenardi C and Gissler W 1996 Ion beam deposited carbon nitride films: characterization and identification of chemical sputtering *Thin Solid Films* **290–291** 107
- [13] Baker M A and Hammer P 1997 Study of the chemical composition and microstructure of ion beam-deposited CN_x films including an XPS C 1s peak simulation *Surf. Interface Anal.* **25** 301
- [14] Baker M A and Hammer P 1997 A study of the chemical bonding and microstructure of ion beam-deposited CN_x films including an XPS C 1s peak simulation *Surf. Interface Anal.* **25** 629
- [15] Hammer P, Victoria N M and Alvarez F 1998 Electronic structure of hydrogenated carbon nitride films *J. Vac. Sci. Technol. A* **16** 2941–9
- [16] Grigull S, Jacob W, Henke D, Mücklich A, Spaeth C and Sümichen L 1997 On the presence of molecular nitrogen in nitrogen-implanted amorphous carbon *Appl. Phys. Lett.* **70** 1387
- [17] Grigull S, Jacob W, Henke D, Spaeth C, Sümichen L and Sigle W 1998 Transport and structural modification during nitrogen implantation of hard amorphous carbon films *J. Appl. Phys.* **83** 5185
- [18] Hammer P and Alvarez F 2001 Influence of chemical sputtering on the composition and bonding of carbon nitride films *Thin Solid Films* **398–399** 116
- [19] Todorov S S, Marton D, Boyd K J, Al-Bayati A H and Rabalais J W 1994 Computer simulation of the ion beam deposition of binary thin films: carbon nitride and boron carbide *J. Vac. Sci. Technol. A* **12** 3192
- [20] Jacob W and Roth J 2007 Chemical sputtering *Sputtering by Particle Bombardment IV (Topics in Applied Physics vol 10)* ed R Behrisch and W Eckstein (Berlin: Springer) pp 329–400

- [21] Grigull S, Behrisch R and Parascandola S 1999 Nitrogen implantation into carbon: retention, release and target-erosion processes *J. Nucl. Mater.* **275** 158
- [22] Hong J and Turban G 1999 Etching process of hydrogenated amorphous carbon (a-C:H) thin films in a dual ECR-rf nitrogen plasma *Diamond Relat. Mater.* **8** 572
- [23] Jacob W, Hopf C and Schlüter M 2005 Chemical sputtering of carbon by nitrogen ions *Appl. Phys. Lett.* **86** 204103
- [24] Roth J and García-Rosales C 1996 Analytic description of the chemical erosion of graphite by hydrogen ions *Nucl. Fusion* **36** 1647–59
Roth J and García-Rosales C 1997 *Nucl. Fusion* **37** 897 (corrigendum)
- [25] Balden M and Roth J 2000 New weight-loss measurements of the chemical erosion yields of carbon materials under hydrogen ion bombardment *J. Nucl. Mater.* **280** 39–44
- [26] Schwarz-Selinger T, Hopf C, Sun C and Jacob W 2007 Growth and erosion of amorphous carbon (a-C:H) films by low-temperature laboratory plasmas containing H and N mixtures *J. Nucl. Mater.* **363–365** 174–8
- [27] Deng Z W and Souda R 2002 Synthesis and thermal decomposition of carbon nitride films prepared by nitrogen ion implantation into graphite *Thin Solid Films* **406** 46–53
- [28] Deng Z W and Souda R 2002 Dynamics of CN^- ion emission during hyperthermal N_2^+ ion irradiation of graphite *Phys. Rev. B* **65** 144108
- [29] Tabarés F L, Rohde V and the ASDEX Upgrade Team 2004 Plasma processing techniques for tritium inventory control in fusion devices *Plasma Phys. Control. Fusion* **46** B381
- [30] Rapp J, Eich T, von Hellermann M, Herrmann A, Ingesson L C, Jachmich S, Matthews G F, Philipps V, Saibene G and contributors to the EFDA-JET Workprogramme 2002 ELM mitigation by nitrogen seeding in the JET gas box divertor *Plasma Phys. Control. Fusion* **44** 639–52
- [31] Rapp J *et al* 2005 Strongly radiating type-III ELMy H-mode in JET an integrated scenario for ITER *J. Nucl. Mater.* **337–339** 826–30
- [32] Tabarés F L, Tafalla D, Tanarro I, Herrero V J, Islyaikin A and Maffiotte C 2002 Suppression of hydrogenated carbon film deposition by scavenger techniques and their application to the tritium inventory control in fusion devices *Plasma Phys. Control. Fusion* **44** L37
- [33] Nagai H, Takashima S, Hiramatsu M, Hori M and Goto T 2002 Behavior of atomic radicals and their effects on organic low dielectric constant film etching in high density N_2/H_2 and N_2/NH_3 plasmas *J. Appl. Phys.* **91** 2615–21
- [34] Jacob W, Hopf C, von Keudell A, Meier M and Schwarz-Selinger T 2003 Particle-beam experiment to study heterogeneous surface reactions relevant to plasma-assisted thin film growth and etching *Rev. Sci. Instrum.* **74** 5123–36
- [35] Jacob W 1998 Surface reactions during growth and erosion of hydrocarbon films *Thin Solid Films* **326** 1
- [36] Schwarz-Selinger T, von Keudell A and Jacob W 1999 Plasma chemical vapor deposition of hydrocarbon films: the influence of hydrocarbon source gas on the film properties *J. Appl. Phys.* **86** 3988
- [37] Eckstein W 1991 *Computer Simulation of Ion–Solid Interactions* 1st edn (*Springer Series in Materials Science*) (Berlin: Springer)
- [38] Hopf C, von Keudell A and Jacob W 2003 Chemical sputtering of hydrocarbon films *J. Appl. Phys.* **94** 2373
- [39] Jacob W, Hopf C and Schlüter M 2006 Chemical sputtering of carbon materials due to combined bombardment by ions and atomic hydrogen *Phys. Scr.* **T124** 32–6
- [40] Schlüter M 2007 Synergismen bei der Erosion von amorphen Kohlenwasserstoffschichten mit niederenergetischen Teilchenstrahlen, eine In-Situ-Ellipsometriestudie *PhD Thesis* University of Bayreuth (in German)
- [41] Ma Y, Foster A S, Krasheninnikov A V and Nieminen R M 2005 Nitrogen in graphite and carbon nanotubes: magnetism and mobility *Phys. Rev. B* **72** 205416
- [42] Hopf C and Jacob W 2005 Bombardment of graphite with hydrogen isotopes: a model for the energy dependence of the chemical sputtering yield *J. Nucl. Mater.* **342** 141

- [43] Hopf C, von Keudell A and Jacob W 2002 Chemical sputtering of hydrocarbon films by low-energy Ar⁺ ion and H atom impact *Nucl. Fusion* **42** L27
- [44] Jacob W, Hopf C, Schlüter M, Schwarz-Selinger T and Chao Sun 2004 Optimisation of hydrocarbon redeposition reduction by tokamak-compatible scavenger techniques *Final Report for EFDA Task TW3-TPP-SCAVOP*, European Fusion Development Agreement (EFDA), December 2004
- [45] Schlüter M, Hopf C, Schwarz-Selinger T and Jacob W 2008 Temperature dependence of the chemical sputtering of amorphous hydrogenated carbon films by hydrogen *J. Nucl. Mater.* **376** 33–7
- [46] Neidhardt J, Högberg H and Hultman L 2005 Cryogenic deposition of carbon nitride thin solid films by reactive magnetron sputtering; suppression of the chemical desorption processes *Thin Solid Films* **478** 34–41
- [47] Hopf C, Schlüter M and Jacob W 2008 Chemical sputtering of a-C:H films by simultaneous exposure to energetic Ar⁺ ions and water vapor *J. Phys.: Conf. Ser.* **100** 062012
- [48] Hopf C, Schlüter M and Jacob W 2007 Chemical sputtering of carbon films by argon ions and molecular oxygen at cryogenic temperatures *Appl. Phys. Lett.* **90** 224106
- [49] Pillath J, Winter J and Waelbroek F 1987 Influence of an a-C:H layer on the gas and plasma driven permeation of hydrogen through iron *Amorphous Hydrogenated Carbon films (E-MRS Symposia Proc. vol XVII)* ed P Koidl and P Oelhafen (Les Ulis: Les Éditions de Physique) p 449
- [50] von Keudell A and Jacob W 1996 Growth and erosion of hydrocarbon films, investigated by *in situ* ellipsometry *J. Appl. Phys.* **79** 1092
- [51] Lide D R (ed) 1994 *Handbook of Chemistry and Physics* vol 75 (Boca Raton, FL: CRC Press)
- [52] Vergara L I, Meyer F W and Krause H F 2005 Chemical sputtering of ATJ graphite induced by low-energy D⁺ bombardment *J. Nucl. Mater.* **347** 118–24
- [53] Meyer F W, Krause H F and Vergara L I 2005 Measurements of chemical erosion of ATJ graphite by low energy D⁺ impact *J. Nucl. Mater.* **337–339** 922–6
- [54] Meyer F W, Vergara L I and Krause H F 2006 Recent ORNL measurements of chemical sputtering of ATJ graphite by slow atomic and molecular D⁺ ions *Phys. Scr.* **T124** 44–9
- [55] Vergara L I, Meyer F W, Krause H F, Träskelin P, Nordlund K and Salonen E 2006 Methane production from ATJ graphite by slow atomic and molecular D ions: evidence for projectile molecule-size-dependent yields at low energies *J. Nucl. Mater.* **357** 9–18
- [56] Yao Y *et al* 1998 New molecular collisional interaction effect in low-energy sputtering *Phys. Rev. Lett.* **81** 550–3
- [57] Hopf C, Schlüter M and Jacob W 2008 Chemical sputtering of carbon films by simultaneous irradiation with argon ions and molecular oxygen *New J. Phys.* submitted